JES Focus Issue on Progress in Molten Salts and Ionic Liquids

Reduction of Solid Al_2O_3 with Electrolysis of $CaCl_2$-Based Melt

A. V. Suzdaltsev,[a,z] A. P. Khramov,[a] Yu. P. Zaikov,[a,b] A. A. Pankratov,[a] E. G. Vovkotrub,[a] and B. D. Antonov[a]

[a]*Institute of High-Temperature Electrochemistry UB RAS, 620137 Yekaterinburg, Russia*
[b]*Ural Federal University, 620002 Yekaterinburg, Russia*

Cyclic and square-wave voltammetry methods are used to investigate the mechanism of the cathode process on molybdenum in a $CaCl_2$-CaF_2 melt at 750°C. It is shown that calcium reduces on an inert cathode in the form of its solution in catholyte at potentials more positive than are required for metallic calcium formation. The presence of Al_2O_3 in the catholyte increases currents of calcium reduction on the forward cathodic wave at potentials more positive than are required for metallic calcium formation. A decrease in the ohmic resistance between the anode and cathode is observed to have been caused by the appearance of electronic conduction during the calcium cathodic reduction in the studied melt. A mechanism for the reduction of Al_2O_3 in the catholyte during electrolysis of the $CaCl_2$-CaF_2 melt, including Ca^+ subions and calcium cathode formation and the secondary reduction of Al_2O_3, is proposed. In order to demonstrate the supposed mechanism for the Al_2O_3 reduction, the electrolysis tests were performed in two laboratory-scale electrolyzers with different separation type of anolyte and catholyte. The necessity of separating the anolyte and catholyte for providing stable continual electrolysis in the $CaCl_2$-based melt is demonstrated.

Manuscript submitted February 14, 2017; revised manuscript received April 28, 2017. Published May 9, 2017. *This paper is part of the JES Focus Issue on Progress in Molten Salts and Ionic Liquids.*

Since Chen and Fray's seminal paper published in 2000[1], over a thousand publications have been devoted to the further development and improvement of direct electroreduction or "electro-deoxidation" of metal oxides in $CaCl_2$-based melts. However, despite this significant attention from researchers from all over the world,[2–5] this promising method is yet to be meaningfully applied at an industrial scale. This is likely to be due to several important mechanisms in the metal oxide reductions remaining to be adequately explained. Thus, in our previous theoretical research,[6] we have shown that non-conductive crystal oxides can be reduced by calcium solution (in a form of Ca, Ca^+ or CaCl) in its chloride.[7–10] The latter can be formed at the inert cathode during electrolysis or due to introduction of calcium metal into the melt. Dissolution of alkali or alkaline earth metal in their halides reveals the nature of such melts, which are representative of ion-electron liquids.[7,8] Therefore, the nature of the melts under study enables using the innovative method only in electrolysis lab tests. Moreover, the presence of calcium (in a form of solution or metal phase) in the molten calcium chloride leads to the appearance of electronic conduction that causes a side reaction of calcium oxidation in the anolyte and at the anode.[11,12]

Since the principal anode material used (as mentioned in most papers[1–5]) is graphite, the discharge of oxygen-containing ions on graphite is accompanied by the formation of anode gases (CO, CO_2) which dissolves in the $CaCl_2$-melts in the form of carbonate ions.[13–16] The latter interact with calcium dissolved in the melt or diffuse to the cathode with subsequent direct discharge to ultrafine carbon.[17,18] Analogously the evolution of CO and CO_2 gases should have affected on the "electro-deoxidation" processes.[1–5] Finally, the presence of carbon in the melt changes its physical-chemical properties, significantly impacting the electrolysis parameters.[19,20] It seems that reactor with a separated anolyte and catholyte required for the electrochemical measurements as well as for electrolysis in the $CaCl_2$-melts. In this case, the mutual influence of the anode and cathode products on the results is minimized. We encountered this problem earlier when studying the anode process on platinum in oxide-fluoride melt.[21]

The aim of this work was to obtain additional experimental data to support a further discussion of the mechanism underlying the processes occurring at the inert cathode in molten $CaCl_2$-CaF_2 containing Al_2O_3 by means of cyclic and square-wave voltammetry as well as electrolysis tests in two laboratory electrolyzers supplied with different types of anolyte-catholyte separation.

Experimental

Melt preparation.—The subject of testing was a (wt%) 80$CaCl_2$-20CaF_2 melt with decreased liquidus temperature and lowered hydrolysis capability in comparison with pure $CaCl_2$.[22] The following individual reagents were used for its preparation: anhydrous $CaCl_2$ and CaF_2 – both chemically pure grade (99.9 wt%, CJSC "Vekton"). The salt mixture was placed in an experimental reactor (alumina crucible) in a closed quartz tube under dry argon atmosphere and gradually heated over a period of 24 hours to an operating temperature of 750°C. The prepared melt was electrolyzed in potentiostatic mode using a molybdenum cathode (99.95 wt%, CJSC "OZTM&TS") and graphite anode (spectral pure grade) with the cathode potential of −2.5 V relative to the CO/CO_2 gas electrode,[23] which was placed in a porous alumina container (open porosity – 1.2 vol. %) together with the (wt%) 80$CaCl_2$-20CaF_2 melt. No oxide was specifically added into the CO/CO_2 gas electrode semi-element electrolyte due to the presence of residual oxygen-containing forms in $CaCl_2$-CaF_2 being taken into account. The duration of the pre-electrolysis was 12–18 hours, with the termination being determined experimentally (with the relative achievement of a current minimum). The melt temperature was regulated by a Varta TP-703 thermocontroller and Chromel-Alumel thermocouple.

Aluminium oxide was chosen as a reducible reagent due to it minor solubility (less than 0.005 wt%) in the melts under study. This data supported by the elemental composition of the metals and alloys sintered by electrolysis of $CaCl_2$-melts in alumina crucibles.[2–5,13,22]

Electrochemical measurements.—The electrochemical measurements were carried out in a closed three-electrode alumina cell in a dry argon atmosphere using a PGSTAT AutoLab 302N and NOVA 1.11 software (Metrom, Netherlands) (with a cell scheme similar to that of the electrolyser presented in Fig. 1). Cyclic and square-wave voltammetry methods were used to determine the features of the cathode processes occurring on the molybdenum substrate. Voltammograms were recorded at potential sweep rates from 0.01 to 1 V s^{-1}. The square-wave voltammograms were recorded at a frequency of 15 Hz and an amplitude of 50 mV. A molybdenum rod (surface area – 1.1 cm^2) served as the working electrode; the counter electrode was

[z]E-mail: suzdaltsev_av@mail.ru

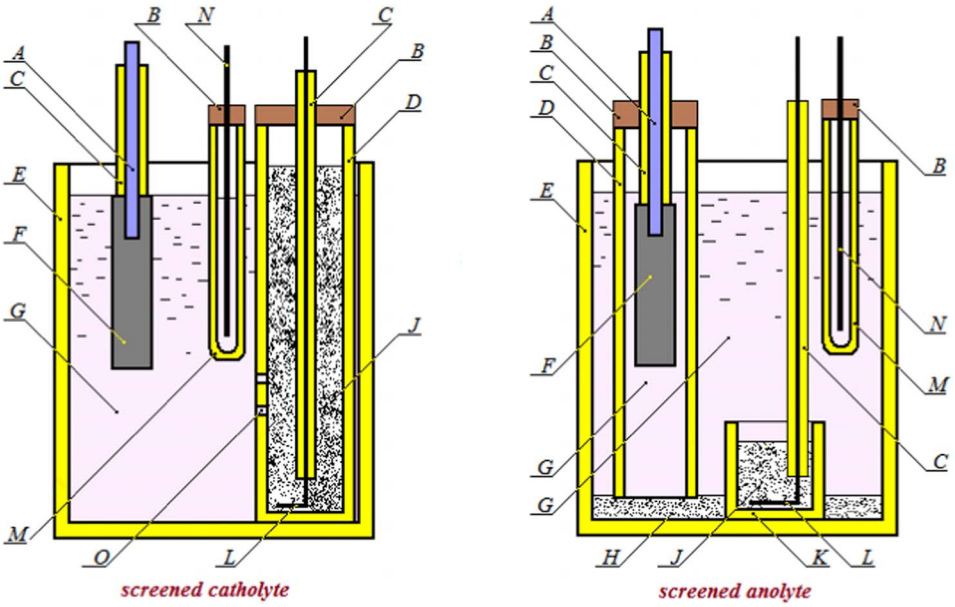

Figure 1. Schemes of reactors for electrochemical measurements and electrolysis tests. *A* – current lead (nichrome); *B* – stoppers (vacuum rubber); *C* – alumina tubes; *D* – alumina tube (diaphragm); *E* – alumina crucible; *F* – anode (spectral pure graphite); *G* – melt; *H* – diaphragm (alumina powder); *J* – Al_2O_3 powder; *K* – alumina crucible; *L* – cathode (molybdenum); *M* – alumina case; *N* – spectral pure graphite (substrate of the CO/CO_2 electrode).

graphite (surface area – 14 cm^2). The gas CO/CO_2 electrode was used as a quasi-reference one.[21] The gas CO/CO_2 electrode was realized by placing the graphite rod (forming the electrode substrate) in the porous sintered alumina case (OJSC "Ogneupory", open porosity – 1.2 vol. %) containing the $CaCl_2$-CaF_2 melt. Due to the Boudouard reaction between the graphite and residual oxygen species in the melt ($CO_2 + C = 2CO$), an equilibrium atmosphere was established and maintained in the alumina container for the duration of the experiment. There were no holes in the alumina container since this function (electron transfer) was performed by the pores. The optimal open porosity value was chosen experimentally. Details of the behavior of the CO/CO_2 gas electrode in oxide-halide melts in terms of potential stability, reproducibility and irreversibility was described in our previous work.[23]

In order to measure and compensate the ohmic resistance (R) of the electric circuit, the current interrupt (I-Interrupt) method was used. The ohmic resistance value was derived from the ohmic drop ($\Delta U = IR$) value, which was typically achieved 2–5 mks after the current (I) interruption. The accuracy of the measured R-values was also checked from the Nyquist plots obtained from the impedance measurements (FRA method).

Electrolysis tests.—Electrolysis of the $CaCl_2$-CaF_2 melt was performed at 750°C in two lab electrolyzers (amperage – 20 A) with different electrode arrangements. Both electrolyzers were placed in a closed quartz tube filled with dried argon. A molybdenum rod (Ø = 1 mm, immersion – 15–40 mm) in an alumina container served as the cathode ***C*** and a dense graphite rod (Ø = 10 mm, immersion – 50 mm) served as the anode. The cathode potential was set relative to the potential of the gas CO/CO_2 electrode.[23] An alumina tube ***D*** (for the both electrolyzers – OJSC "Ogneupory"; inner diameter – 18 mm; thickness – 3 mm; open porosity – 0.5 vol.%) was used to separate the anolyte and catholyte. In the first construction (Fig. 1, left) the cathode and Al_2O_3 powder (8 g) were placed into the alumina tube; two holes (Ø = 0.5 mm) were made to provide a passage for the electrical current. In a second construction the electric current was passed through the layer of Al_2O_3 powder at the bottom of alumina container. The alumina tube ***D*** was immersed in the Al_2O_3 layer, which provided a good separation of the anolyte and catholyte in this construction. The molybdenum cathode and Al_2O_3 powder (8 g) were placed in an alumina crucible (Fig. 1).

Pre-electrolysis.—The voltammograms obtained on molybdenum with a potential scan rate of 0.1 V s^{-1} after melt preparation (curve 1) and following pre-electrolysis (curve 2) for 2 hours at cathode potential $E_{Mo} \approx 0.9$ V (recalculated against the potential of saturated calcium electrode) are presented in Fig. 2. The peak at the cathode potential $E_{Mo} \approx 1.8 \ldots 2.4$ V is apparently associated with the discharge of the residual hydrogen, which presented itself in the form of hydrolysis products ($Ca(OH)_2$, Ca(OH)Cl and others[24]). The discharge in the measuring cell with the CO/CO_2 electrode can be described as follows:

$$Ca(OH)_2 + \frac{1}{1+x} = \frac{1-x}{1+x}CO + \frac{x}{1+x}CO_2 + H_2 + CaO \qquad [1]$$

where x is the volume fraction of CO_2 in the semi-element of the reference electrode, which corresponds to the equilibrium of the Boudouard reaction at certain temperature, (1-x) is the volume fraction of CO. Evaluation of the hydrogen discharge potential according this Reaction 1 is complicated because of the unknown activities of $Ca(OH)_2$ and CaO and partial pressure of H_2 in the semi-element of the working electrode.

In our previous experience with the CO/CO_2-electrodes,[23] we have been able to achieve stable, reproducible potential even while utilizing simple manufacturing techniques. We use electrodes of this type in present study for these reasons. It is not possible to carry out thermodynamic calculations in accordance with reactions of type (1) using the CO/CO_2 electrode. The potential of the CO/CO_2 electrode was estimated experimentally against the potential of the saturated calcium electrode. The saturated calcium electrode consists of calcium supplied with the molybdenum rod as a sensor of its electrical potential. In our experiments it's a (dynamic) working electrode, on which the calcium mole-fraction activity is closed to (1) due to the high cathode current density. Further, all potentials were recalculated against the potential of the saturated calcium electrode (marked on the graphs as a dashed line). An analogous approach was used by Bard.[25]

Following pre-electrolysis, the peak value decreased from 0.33 to 0.16 A cm^{-2}.

Analysis of melt and synthesis products.—In order to determine the peculiarities of the Al_2O_3 reduction mechanism, the composition of the products in the catholyte and pores of the alumina tube were analyzed by means of Raman spectroscopy (RAMAN), X-ray diffraction (XRD) and scanning electron microscopy (SEM + EDX) methods. The following equipment was used: Renishaw U 1000 Raman microscope-spectrometer (Renishaw, UK); Rigaku D/MAX-2200VL/PC automatic X-ray diffractometer (Rigaku, Japan); JEOL X-act ADD + JSM-5900LV scanning electron microscope with

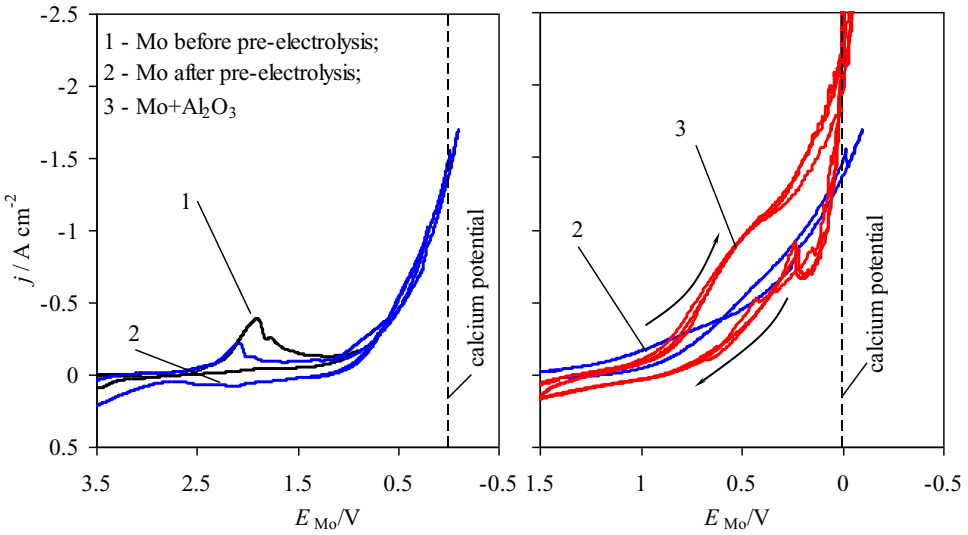

Figure 2. Voltammograms, obtained on molybdenum in the $CaCl_2$-CaF_2 melt at 750°C and a potential sweep rate of 0.1 V s^{-1} without (curves 1, 2) and with Al_2O_3 powder (curve 3) in the catholyte. Gas CO/CO_2 quasi-reference electrode.

nitrogen-free energy dispersive detector (JEOL, Japan) supplied with a wave dispersive micro analyzer, sluice chamber and INCA Energy 250 and INCA Wave500 devices for suppression of electromagnetic interference (Oxford Instruments, UK).

Results and Discussion

Kinetics of the cathode process.—A gradual increase in the cathodic current density from the potential of about 0.9 V and its sharp increase at the potential range of 0.1 . . . 0.0 V is observed on the voltammogram obtained on molybdenum in the $CaCl_2$-CaF_2 melt without Al_2O_3 in the catholyte (Fig. 2, curve 2). Such a course of the non-stationary *i-E* dependence confirms the results of stationary polarization studies[26] on inert cathodes in the $CaCl_2$-KCl melt. Analysis of stationary polarization curves revealed that a number of electrons of the cathode process occurred at more positive potentials than calcium metal reduction is equal to one.[26] This process can be explained by the formation of the calcium subions solution in calcium chloride:[6]

$$Ca^{2+} + e \rightarrow Ca^{+} \qquad [2]$$

A similar mechanism of the process is observed during cathodic reduction of alkali and alkaline earth metals.[27]

The addition of non-conductive insoluble oxide powder (Al_2O_3)[13] into the catholyte leads to an additional rising of the cathode currents at potentials more negative than 0.9 V. In our opinion, this happens due to the fact that cathodically formed Ca^+ (in the form of calcium sub-chloride CaCl[9,10]) can be consumed in the catholyte by oxide, for example, according to reaction:

$$Al_2O_3 + 6CaCl \rightarrow 2Al + 3CaO + 3CaCl_2 \qquad [3]$$

This leads to a kinetic increase in cathodic Reaction 2 currents during the non-steady experiment at potentials more positive than the thermodynamic potential of the calcium metal formation. Such an interpretation of the reduction mechanism of oxides to metals in the $CaCl_2$-based melts at cathode potentials more positive than the potential of the metal calcium formation is consistent with the results of electrolysis tests described in previous works.[1–5,25]

An increase in the potential sweep rate to 5 V s^{-1} results in an increase in the cathodic current in the potential range of 0.9. . . 0.1 V (Fig. 3) even while the features of the solid oxide reduction peaks remain the same (increased cathode currents on the right semi-waves of voltammograms). In accordance with these observations, we think it likely that the subsequent chemical Reaction 3 limits the summary process in the melt under study even at high solubility of CaO in the $CaCl_2$-based melts.[28] This can explained by limitations in CaO (or O^{2-} anions) transfer from the reducible oxide into the melt though a sponge layer of reduced metal, pores and capillaries which are, most probably, filled with double oxides and melt saturated with CaO. Moreover the presence of a double oxide in pores can complicates both the removal of CaO and admission of reductant (electrons from the Ca^+ cations) to the reaction front of oxide reduction. This assumption has been confirmed by the electrolysis tests performed using lab scale electrolyzers having different catholyte arrangements.

In order to clarify features of the cathode process square-wave voltammetry was also used. The typical square-wave voltammograms obtained on molybdenum with and without Al_2O_3 powder in the catholyte are demonstrated in Fig. 4. One can see two precise peaks at the cathode potentials of about 0.75 and 0.30 V. Wherein peaks

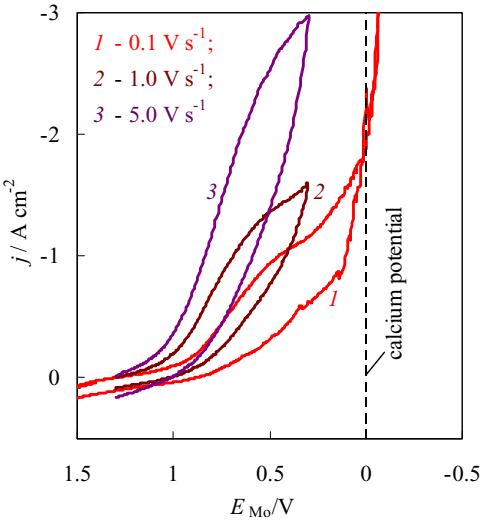

Figure 3. Voltammograms, obtained on molybdenum in the $CaCl_2$-CaF_2 melt at 750°C and potential sweep rates of 0.1–5.0 V s^{-1} with the Al_2O_3 powder in the catholyte. Gas CO/CO_2 quasi-reference electrode.

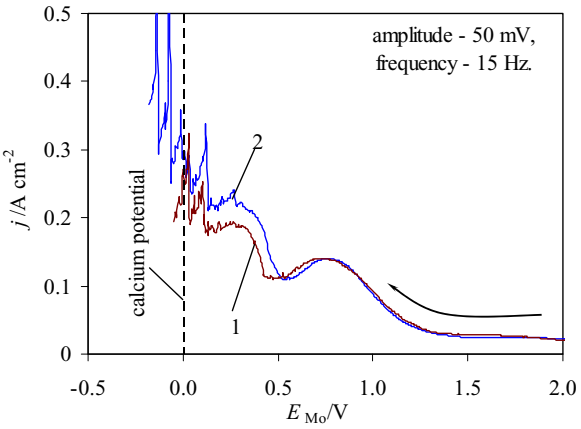

Figure 4. Square-wave voltammograms, obtained on molybdenum in the $CaCl_2$-CaF_2 melt at 750°C without (curves 1) and with the Al_2O_3 powder (curve 2) in the catholyte. Gas CO/CO_2 quasi-reference electrode.

occur at voltammogram obtained in a melt without the Al_2O_3 powder. This suggests that process (2) takes place at the potential of 0.75 V, and the electroreduction of Ca^+ subions to calcium thorough the reaction

$$Ca^+ + e \rightarrow Ca \qquad [4]$$

takes place at the potential of 0.30 V. One can see the wave of metal calcium formation at cathode potentials more negative than minus 0.1 V, which are accompanied by fluctuations of the measured current. We explain this feature in terms of the formation of an ion-electron liquid in a catholyte saturated with Ca^+ subions.[7–10] The geometry (geometric shape and surface area of the region where an ion-electron liquid distributed) of the latter is variable because of the parallel processes in the catholyte: cathodic formation of the Ca^+ subions and their consumption due to migration into the melt or due to the preceding Reaction 6. This leads to fluctuations in the real cathode-melt interface.

Electrolysis tests.—Formation of Ca^+ subions by Reaction 2 or by reaction:[5,6]

$$Ca + CaCl_2 \rightarrow 2CaCl. \qquad [5]$$

was observed during the preliminary electrolysis tests in the electrolyser as shown in Fig. 1 (left). The latter leads to the appearance of the electronic component of the common conductivity of the investigated melt.[6,7]

Even small amounts of passed current (0.1–0.4 A · h) decrease the melt electroresistance from 1.5–2.3 to 0.15–0.22 Ohms in our experiments. Therefore, a correction (especially at the initial stage) of the compensated electroresistance should be carried out for stable organization of the potentiostatic electrolysis of the $CaCl_2$-based melts with a relatively constant cathode potential value. Otherwise, overcompensation can occur. Taking this into account, stable potentiostatic (E_{Mo} = 0.6. . . .0.4 V) and galvanostatic electrolysis (at cathode current densities up to 1 A cm^{-2}) was performed in both electrolyzers (Fig. 1). During the galvanostatic electrolysis the cathode current was adjusted in such a way that the cathode potential ranged between 0.6 and 0.4 V (not including the ohmic drop).

Electrolysis with screened catholyte.—The cathode current density was varied in the range of 0.05–0.20 A cm^{-2} during the 24-hour potentiostatic electrolysis of the $CaCl_2$-CaF_2 melt in the electrolyser with screened catholyte containing the molybdenum cathode and the Al_2O_3 powder (Fig. 1, left). The electrolysis was periodically stopped in order to adjust the compensated ohmic resistance of the circuit.

Next, the electrolysis reactor was cooled under inert atmosphere and autopsied. A greying of the alumina tube ***D*** (in its longitudinal shear) and a black amorphous deposit in the holes was observed. The majority of the Al_2O_3 powder in the alumina tube (in the catholyte) remained white. Only the Al_2O_3 powder in the region between the molybdenum cathode and holes in the alumina tube became gray. We assume that the Al_2O_3 powder in this region was partially reduced to the conductive double oxide $Al_2O_3{}^*nCaO$[29,30] during the passage of the electric current. After that, it began to perform the function of transmitting current to the cathode, which organized on the external surface of the holes in the alumina tube. This led to a local increase in the current density of the actual cathode and to the formation of calcium. The latter then reacted with the carbon-containing ions dissolved in the melt to form ultrafine carbon[17,18] on the holes of the alumina tube.

According to the analysis (XRD, SEM + EDX), the black deposition in holes consisted of ultrafine carbon and the dark gray area comprised a mixture of Al_2O_3 and $Ca_{12}Al_{14}O_{33}$ oxides. The metal phase was not found in the electrolyser.

Similar results were observed after the 18-hour galvanostatic electrolysis with a cathode current density between 0.2 and 0.5 A cm^{-2}.

Electrolysis with screened anolyte.—The electrolysis tests were carried out in the electrolyser with a graphite anode (Fig. 1, right). The alumina tube ***D*** served as a separator between the anolyte and catholyte. Both potentiostatic (at E_{Mo} = 0.60. . . 0.40 V for 24 hours) and galvanostatic (at a cathode current density of 0.5 A cm^{-2} for 18 hours) modes were applied.

Droplets of the metal phase (Ø = 1–4 mm) were observed on the bottom of the alumina crucible following electrolysis (Fig. 5d). The alumina tube ***D*** became gray (Fig. 5b) as was the case with electrolysis carried out in a different electrolyser. Traces of the metal phase (aluminum) were also observed on the shear surface of the alumina tube ***D*** (Fig. 5c, 50 times magnification). Features of the investigated processes were reproduced in a few experiments.

The RAMAN and XRD analysis of the different parts of electrolyser after the electrolysis (alumina tube, metal, and an undissolved

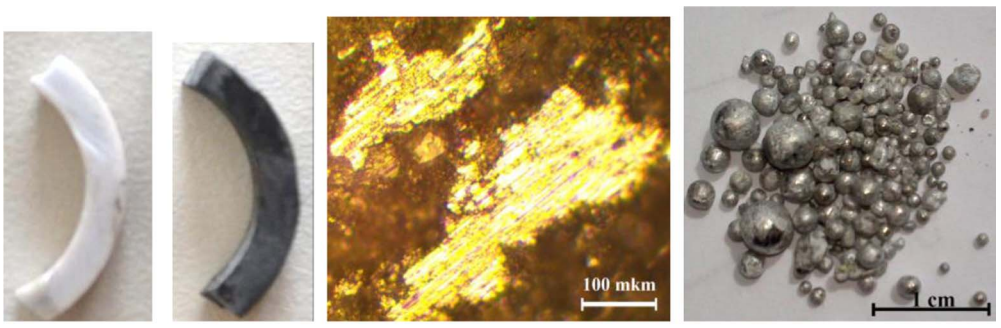

Figure 5. Photos / SEM images of the alumina tube (thickness - 3 mm) before (a) and after the electrolysis (b, c), and metal droplets after the electrolysis (d).

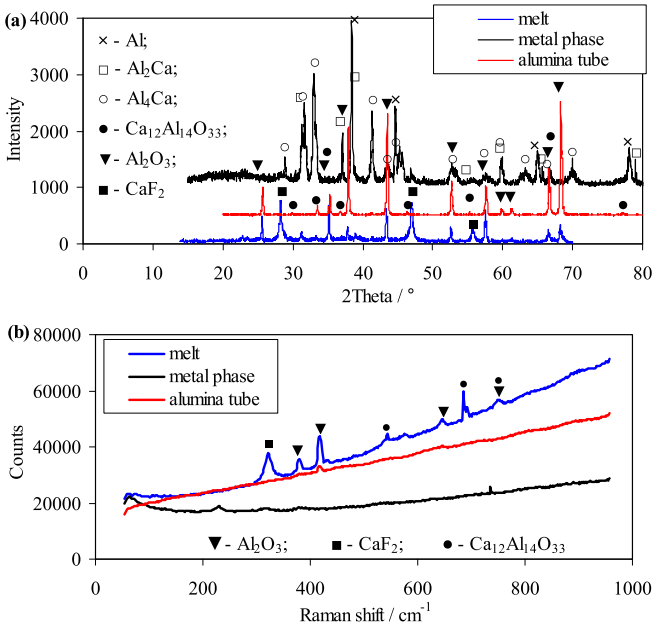

Figure 6. XRD (a) and RAMAN (b) analysis of the compositions of the different phases after the potentiostatic electrolysis (at $E_{Mo} = 0.6 \ldots .0.4$ V during 24 hours)) of the $CaCl_2$-CaF_2 melt at 750°C with the screened anolyte and Al_2O_3 powder in the catholyte.

part of the melt after its washing in distilled water) are given in Fig. 6. One can see the phases of $Ca_{12}Al_{14}O_{33}$, CaF_2, and Al_2O_3 in the melt as well as in the alumina tube. The phases of Al, Al_2Ca, Al_4Ca were obtained in the metal droplets. The absence of intermediate CaCl is associated with its instability,[8,9] as well as with the fact that the analyses were not carried out in situ in the molten state. The presence of metallic calcium (in the intermetallic compounds) may be caused both by the Reaction 5 and by the direct calcium discharge at the cathode with the depolarization. In the case of electrolysis, the depolarization can be caused by the formation of alloys (Al_2Ca, Al_4Ca).[31,32]

The obtained results confirm the presence of the subsequent chemical reaction, which can limit the summary process in the case of the electrolyser with the screened catholyte.

Based on the electrochemical measurement and electrolysis tests, the formation mechanism of aluminum and its alloys from Al_2O_3 during the electrolysis of the $CaCl_2$-based melts can be described as follows. Calcium (Ca^+, Ca) discharges on the cathode and reduces the Al_2O_3 powder in the catholyte thorough the reactions:

$$Al_2O_3 + 6CaCl \rightarrow 2Al + 3CaO + 3CaCl_2, \quad [6]$$

$$11Al_2O_3 + 24\,Cl \rightarrow 8Al + Ca_{12}Al_{14}O_{33} + 12\,Cl_2, \quad [7]$$

$$Al_2O_3 + 3Ca \rightarrow 2Al + 3CaO, \quad [8]$$

$$11Al_2O_3 + 12 \rightarrow 8Al + Ca_{12}Al_{14}O_{33} \quad [9]$$

Less probable is the formation of $Ca_{12}Al_{14}O_{33}$ by the following reaction:

$$7Al_2O_3 + 12CaO \rightarrow Ca_{12}Al_{14}O_{33} \quad [10]$$

The photography of the metal phase droplets and microphotography (SEM) of the shear of the alumina tube following their holding in air are presented in Fig. 7. It can be seen that the obtained products (Al, Al_2Ca, Al_4Ca), whether as a separate phase or in the pores of the alumina tube, are oxidized. This fact should be taken into account when developing technology for the production of aluminium-calcium alloys using the studied methodological approach. Loosening of the metal droplets due to their oxidation in air indicates that chemically active calcium has a uniform distribution in the alloy matrix.

It should also be noted that uniform inclusions of the carbon-containing component are present in pores of the alumina tube (Fig. 7c). This can indicate the dissolution of the anode gases CO and CO_2 in the melt with the formation of carbonate ions.

The obtained results confirm the possibility in principle of aluminium-calcium alloy production through electrolysis of the $CaCl_2$-based melts using an electrolyser with separated anolyte and catholyte. However, a systematic study of the synthesis parameters is required in order to develop the necessary technology for their production.

Conclusions

The kinetics of the cathodic formation of calcium in the $CaCl_2$-CaF_2 melt at 750°C was studied by means of cyclic and square-wave voltammetry. It was revealed that the formation of calcium takes place at potentials more positive than the thermodynamic potential of the metallic calcium formation. The presence of the Al_2O_3 powder in the catholyte leads to the subsequent chemical reaction of the consumption of the reduced forms of calcium (Ca^+, Ca). The increase in the cathode current confirms this statement.

In order to demonstrate the features of the suggested Al_2O_3 reduction mechanism in the $CaCl_2$-CaF_2 melt at 750°C, the electrolysis tests were performed in two electrolyzers with different approaches to separating the anolyte and the catholyte. Based on the analysis of the electrolysis products, the synthesis mechanism of aluminum and its alloys during the electrolysis of $CaCl_2$-based melts was described. The possibility in principle of the production of aluminium-calcium alloys using an electrolyser with graphite anode was demonstrated and the main features of this process described.

References

1. G. Z. Chen and D. J. Fray, *Nature*, **407**, 361 (2000).
2. D. Wang, X. Jin, and G. Z. Chen, *Annual Reports Section "C"*, **104**, 189 (2008).
3. A. M. Abdelkader, K. T. Kilby, A. Cox, and D. J. Fray, *Chem. Reviews*, **113**, 2863 (2013).
4. J. Peng, G. Li, H. Chen, D. Wang, X. Jin, and G. Z. Chen, *J. Electrochem. Soc.*, **157**, F1 (2010).

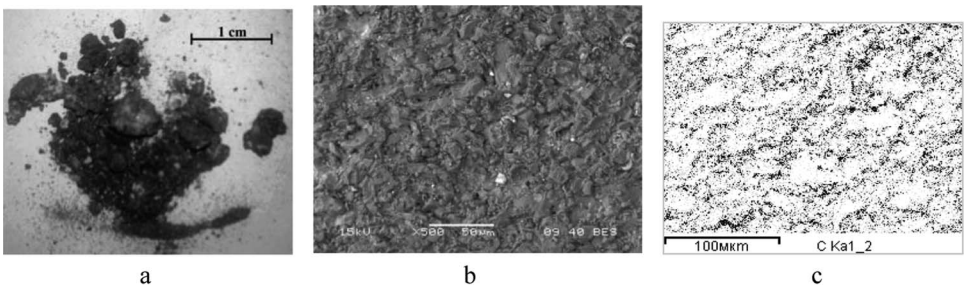

Figure 7. Photography of the oxidized metal droplets (a), microphotography (SEM) of the shear of the alumina tube after their holding in air (b) and carbon distribution in alumina tube (c).

5. J. Cai, X. Luo, G. M. Haarberg, O. E. Kongstein, and Sh. Wang, *J. Electrochem. Soc.*, **159**(3) D155 (2012).
6. N. I. Shurov, A. P. Khramov, Yu. P. Zaikov, V. A. Kovrov, and A. V. Suzdaltsev, *Rus. J. Non-Ferrous Metals*, **56**, 267 (2015).
7. A. S. Dworkin, H. R. Bronstein, and M. A. Bredig, *Discuss. of Faraday Society*, **32**, 188 (1961).
8. J. Sytchev and G. Kaptay, *Electrochim. Acta*, **54**, 6725 (2009).
9. P. J. Dagdigian, *Chem. Physics*, **21** 453 (1977).
10. J. Benhelm, G. Kirchmair, C. F. Roos, and R. Blatt, *Nature Physics*, **4**, 463 (2008).
11. Yu. P. Zaikov, N. I. Shurov, and A. V. Suzdaltsev, *High-temperature electrochemistry of calcium (Vysokotemperaturnaya elektrokhimiya kaltsiya)*, Yekaterinburg: EPD UB RAS (2013).
12. M. A. Bredig, In *Molten Salts Chemistry*, M. Blender, Ed., New York: Interscience, 367 (1964).
13. V. A. Lebedev, V. I. Salnikov, M. V. Tarabaev, I. A. Sizikov, and D. A. Rymkevich, *Rus. J. Applied Chemistry*, **80**, 1498 (2007).
14. Yo. Sakamura and M. Iizuka, *Electrochim. Acta*, **189**, 74 (2016).
15. V. Tomkute, A. Solheim, and E. Olsen, *Energy Fuels*, **28**, 5345 (2014).
16. I. A. Novoselova, S. V. Kuleshov, S. V. Volkov, and V. N. Bykov, *Electrochimica Acta*, **211**, 343 (2016).
17. K. Otake, H. Kinoshita, T. Kikuchi, and R. O. Suzuki, *Electrochim. Acta*, **100**, 293 (2013).
18. L. Li, Zh. Shi, B. Gao, J. Xu, X. Hu, and Zh. Wang, *Electrochemistry*, **82**, 1072 (2014).
19. N. A. Doronin, *Kaltsiy (Calcium)*, Moscow: Gosatomizdat, 1962.
20. J. Thonstad, P. Fellner, G. M. Haarberg et al.: *Aluminum Electrolysis. Fundamentals of the Hall-Héroult Process*, 3rd ed. by Aluminum-Verlag Marketing & Kommunikation GmbH (2001).
21. V. N. Nekrasov, O. V. Limanovskaya, A. V. Suzdaltsev, A. P. Khramov, and Yu. P. Zaikov, *Rus. Metallurgy*, **8**, 664 (2014).
22. Yu. P. Zaikov, A. P. Khramov, V. P. Batukhtin, L. E. Ivanovskiy et al. In *Proc. of the NATO Adv. Research Workshop on Refractory Metals in Molten Salts*, ed. by D. H. Kerridge and E. G. Polyakov. Kluwer Academic Publishers, Netherlands, **53**, 197 (1998).
23. A. V. Suzdaltsev, A. P. Khramov, and Yu. P. Zaikov, *Rus. J. Electrochem.*, **48**, 1141 (2012).
24. Yu. P. Zaikov, V. P. Batukhtin, N. I. Shurov, L. E. Ivanovskii, and A. V. Suzdaltsev, *Met. & Mat. Trans. B*, **45**, 961 (2014).
25. S. K. Cho, F. F. Fan, and A. J. Bard, *Electrochim. Acta*, **65**, 57 (2012).
26. A. G. Sychev, N. A. Nikulin, Yu. P. Zaikov, and L. E. Ivanovskii, *Rasplavy (Melts)*, **6**, 32 (1992).
27. A. N. Baraboshkin, *Electrocrystallizatoin of Metals from Molten Salts (Elektrokristallizatsiya metallov iz rasplavlennykh solei)*, Moscow: Nauka (1976).
28. G. S. Perry and L. G. MacDonald, *J. Nucl. Mat.*, **130**, 234 (1985).
29. D. S. Tsvetkov, A. S. Steparuk, and A. Yu. Zuev, *Solid State Ionics*, **276**, 142 (2015).
30. M. Lacerda, A. R. West, and J. T. S. Irvine, *Solid State Ionics*, **59**, 257 (1993).
31. E. T. Turkdogan, *Physical Chemistry of High-Temperature Technology*, Academic Press, NY (1980).
32. *JANAF Thermochemical Tables,* 2ed. US Bureau stand., NSRD. Wash. (1971).